

7 Wilson Coefficients and Hard Dynamics

We now turn to the dynamics of SCET at one loop. An interesting aspect of loops in the effective theory is that often a full QCD loop graph has more than one counterpart with similar topology in SCET. We will compare the SCET one loop calculation for a single hard interaction current with the one loop calculation in QCD. Our goal is to understand the IR and UV divergences in SCET and the corresponding logarithms, as well as understanding how the terms not associated to divergences are treated.

In our analysis we will use the same regulator for infrared divergences, and show that the IR divergences in QCD and SCET exactly agree, which is a validation check on the EFT. The difference determines the Wilson coefficient for the SCET operator that encodes the hard dynamics. This matching result is independent of the choice of infrared regulator as long as the same regulator is used in the full and effective theories. Finally, the SCET calculation contains additional UV divergences, beyond those in full QCD, and the renormalization and anomalous dimension determined from these divergences will sum up double Sudakov logarithms.

We will give two examples of matching QCD onto SCET, the $b \rightarrow s\gamma$ transition, and $e^+e^- \rightarrow 2$ -jets. The first example has the advantage of involving only one collinear sector, but the disadvantage of requiring some familiarity with Heavy Quark Effective theory for the treatment of the b quark and involving contributions from two Dirac structures. The second example only involves jets with a single Dirac structure, but has two collinear sectors. In both cases we will use Feynman gauge for all gluons, and dimensional regularization with $d = 4 - 2\epsilon$ for all UV divergences (denoting them as $1/\epsilon$). To regulate the IR divergences we will take the strange quark offshell, $p^2 \neq 0$. For IR divergences associated purely with the heavy quark we will use dimensional regularization (denoting them $1/\epsilon_{\text{IR}}$ to distinguish from the UV divergences).

7.1 $b \rightarrow s\gamma$, SCET Loops and Divergences

As a 1-loop example consider the heavy-to-light currents for $b \rightarrow s\gamma$. Although there are several operators in the full electroweak Hamiltonian, for simplicity we will just consider the dominant dipole operator $J_{\mu\nu}^{\text{QCD}} F^{\mu\nu}$ where $F_{\mu\nu}$ is the photon field strength and the quark tensor current is

$$J^{\text{QCD}} = \bar{s} \Gamma b, \quad \Gamma = \sigma^{\mu\nu} P_R. \quad (7.1)$$

In SCET the corresponding current (for the original Lagrangian, prior to making the Y_n field redefinition) was

$$J^{\text{SCET}} = (\bar{\xi}_n W) \Gamma h_v C(v \cdot n \bar{\mathcal{P}}^\dagger) = \int d\omega C(\omega) \bar{\chi}_{n,\omega} \Gamma h_v. \quad (7.2)$$

In general because of the presence of the vectors v^μ and n^μ there can be a larger basis of Dirac structures Γ for the SCET current (we will see below that at one-loop there are in fact two non-zero structures for the SCET tensor current). Note that the factor of $v \cdot n$ makes it clear that the current preserves type-III RPI. We will set $v \cdot n = 1$ in the following.

Together with the QCD and (leading order) SCET Lagrangians, we can carry out loop calculations with these two currents. First lets consider loop corrections in QCD. We have a wavefunction renormalization graph for the heavy quark denoted b , and one for the massless (strange) quark denoted q :



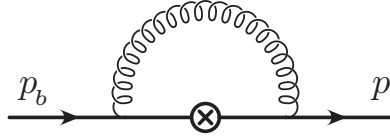
This gives the wavefunction renormalization factors Z_{ψ_b} and Z_ψ respectively. In the ‘‘on-shell’’ scheme which includes both the UV divergences and the finite residues these Z -factors are

$$\begin{aligned} Z_{\psi_b} &= 1 - \frac{\alpha_s C_F}{4\pi} \left[\frac{1}{\epsilon} + \frac{2}{\epsilon_{\text{IR}}} + 3 \ln \frac{\mu^2}{m_b^2} + 4 \right], \\ Z_\psi &= 1 - \frac{\alpha_s C_F}{4\pi} \left[\frac{1}{\epsilon} - \ln \frac{-p^2}{\mu^2} + 1 \right]. \end{aligned} \quad (7.3)$$

(If one instead uses $\overline{\text{MS}}$ for the wavefunction renormalization factors, then the finite residues still show up in the final result for the S-matrix element due to the LSZ formula.) The remaining diagram is a vertex graph for the tensor current J^{QCD} . At tree level the matrix element gives

$$V_{\text{qcd}}^0 = \bar{u}_s(p) P_R i\sigma^{\mu\nu} u_b(p_b) \quad (7.4)$$

while the one-loop diagram



gives

$$\begin{aligned} V_{\text{qcd}}^1 &= -\frac{\alpha_s C_F}{4\pi} \left[\ln^2 \left(\frac{-p^2}{m_b^2} \right) + 2 \ln \left(\frac{-p^2}{m_b^2} \right) - \frac{2}{\epsilon} + \frac{1}{2} \ln \left(\frac{-p^2}{\mu^2} \right) + 2 \ln \frac{\mu}{\omega} - 3 \ln \frac{\mu}{m_b} + f_1(1 - \hat{q}^2) \right] \bar{u}_s P_R i\sigma^{\mu\nu} u_b \\ &+ \frac{\alpha_s C_F}{4\pi} f_2(1 - \hat{q}^2) \bar{u}_s P_R \left(\frac{p^\mu \gamma^\nu - p^\nu \gamma^\mu}{m_b} \right) u_b, \end{aligned} \quad (7.5)$$

where we have kept $p^2 \neq 0$ only for the IR singularities, and set it to zero whenever it is not needed to regulate an IR divergence. The variable $\hat{q}^2 = (p_b - p)^2/m_b^2 = 1 - 2p_b \cdot p/m_b^2$ and the functions appearing in Eq. (7.5) are

$$f_1(x) = \ln(x) + \frac{2}{(1-x)} \ln(x) + 2\text{Li}_2(1-x) + \pi^2, \quad f_2(x) = \frac{4}{(1-x)} \ln(x). \quad (7.6)$$

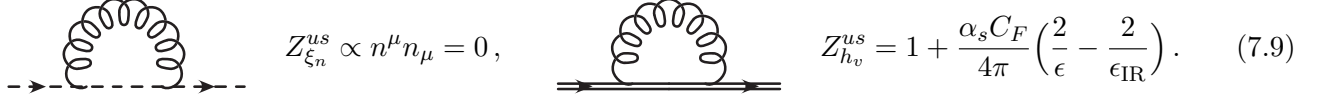
Unlike for the conserved vector current, in QCD for the tensor current the sum of vertex and wavefunction graphs still contains a $1/\epsilon$ UV divergence. Hence this QCD local current operator requires an additional counterterm not related to strong coupling renormalization, and it is given by

$$Z_{\text{tensor}} = 1 + \frac{\alpha_s C_F}{4\pi} \frac{1}{\epsilon}. \quad (7.7)$$

Adding together the QCD vertex graph and the contributions from the three Z 's, and replacing the kinematic variable $\hat{q}^2 = 1 - \bar{n} \cdot p/m_b = 1 - \omega/m_b$, the sum gives

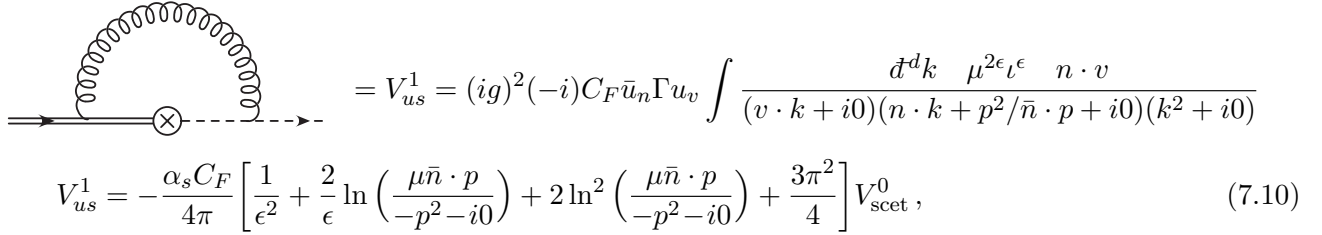
$$\begin{aligned} \text{QCD Sum} &= V_{\text{qcd}}^1 + \left[\frac{1}{2}(Z_{\psi_b} - 1) + \frac{1}{2}(Z_\psi - 1) + (Z_{\text{tensor}}^{-1} - 1) \right] V_{\text{qcd}}^0 \\ &= -\bar{u}_s \Gamma u_b \frac{\alpha_s C_F}{4\pi} \left[\ln^2 \left(\frac{-p^2}{\omega^2} \right) + \frac{3}{2} \ln \left(\frac{-p^2}{\omega^2} \right) + \frac{1}{\epsilon_{\text{IR}}} + \ln \left(\frac{\mu^2}{\omega^2} \right) + f_1 \left(\frac{\omega}{m_b} \right) + \frac{5}{2} \right] \\ &+ \frac{\alpha_s C_F}{4\pi} f_2 \left(\frac{\omega}{m_b} \right) \bar{u}_s P_R \left(\frac{p^\mu \gamma^\nu - p^\nu \gamma^\mu}{m_b} \right) u_b, \end{aligned} \quad (7.8)$$

Next consider the ultrasoft loops in SCET. In Feynman gauge the ultrasoft wavefunction renormalization of the collinear quark vanishes, since the couplings are both proportional to n^μ , and $n^2 = 0$. The ultrasoft wavefunction renormalization of the heavy quark is just the HQET wavefunction renormalization. We summarize these two results as:



$$Z_{\xi_n}^{us} \propto n^\mu n_\mu = 0, \quad Z_{h_v}^{us} = 1 + \frac{\alpha_s C_F}{4\pi} \left(\frac{2}{\epsilon} - \frac{2}{\epsilon_{\text{IR}}} \right). \quad (7.9)$$

We can already note that the $1/\epsilon_{\text{IR}}$ pole in $Z_{h_v}^{us}$ matches up with the IR pole in Z_{ψ_b} in full QCD (and this is the only IR divergence that we are regulating with dimensional regularization). In addition to wavefunction renormalization there is an ultrasoft vertex diagram for the SCET current. Using the on-shell condition $v \cdot p_b = 0$ for the incoming b -quark, and the SCET propagator from Eq. (4.43) for a line with injected ultrasoft momentum, we have



$$V_{us}^1 = (ig)^2 (-i) C_F \bar{u}_n \Gamma u_v \int \frac{\bar{d}^d k \mu^{2\epsilon} \iota^\epsilon n \cdot v}{(v \cdot k + i0)(n \cdot k + p^2/\bar{n} \cdot p + i0)(k^2 + i0)}$$

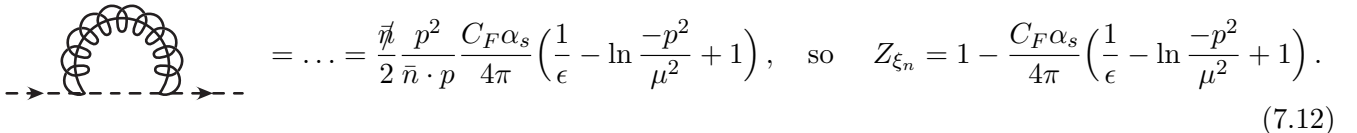
$$V_{us}^1 = -\frac{\alpha_s C_F}{4\pi} \left[\frac{1}{\epsilon^2} + \frac{2}{\epsilon} \ln \left(\frac{\mu \bar{n} \cdot p}{-p^2 - i0} \right) + 2 \ln^2 \left(\frac{\mu \bar{n} \cdot p}{-p^2 - i0} \right) + \frac{3\pi^2}{4} \right] V_{\text{scet}}^0, \quad (7.10)$$

where the tree level SCET amplitude is

$$V_{\text{scet}}^0 = \bar{u}_n \Gamma u_v, \quad (7.11)$$

and $\iota^\epsilon = (4\pi)^{-\epsilon} e^{\epsilon\gamma_E}$ ensures that the scale μ has the appropriate normalization for the $\overline{\text{MS}}$ scheme. Note that this graph is independent of the current's Dirac structure Γ . On the heavy quark side the heavy-quark propagator gives a $P_v = (1 + \not{v})/2$, but this commutes with the HQET vertex Feynman rule and hence yields a projector on the HQET spinor, $P_v u_v = u_v$. On the light quark side the propagator gives a $\not{\bar{n}}/2$ and the vertex gives a $\not{\bar{n}}/2$ to yield the projector $P_n = (\not{\bar{n}}\not{\gamma})/4$ acting on the light-quark spinor, $P_n u_n = u_n$. Hence whatever Γ is inserted at the current vertex is also the Dirac structure that appears between spinors in the answer for the loop graph. For this heavy-to-light current this feature is actually true for all loop diagrams in SCET, the spin structure of the current is preserved by loops diagrams in the EFT. For ultrasoft diagrams it happens by a simple generalization of the arguments above, while for collinear diagrams the interactions only appear on the collinear quark side of the Γ , so we just need to know that they do not induce additional Dirac matrices. (This is ensured by chirality conservation in the EFT.)

Lets finally consider the one loop diagrams with a collinear gluon. There is no wavefunction renormalization diagram for the heavy quark, since the collinear gluon does not couple to it. There is a wavefunction renormalization graph for the light-collinear quark



$$= \dots = \frac{\not{\bar{n}} p^2}{2 \bar{n} \cdot p} \frac{C_F \alpha_s}{4\pi} \left(\frac{1}{\epsilon} - \ln \frac{-p^2}{\mu^2} + 1 \right), \quad \text{so} \quad Z_{\xi_n} = 1 - \frac{C_F \alpha_s}{4\pi} \left(\frac{1}{\epsilon} - \ln \frac{-p^2}{\mu^2} + 1 \right). \quad (7.12)$$

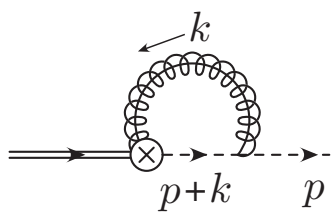
We have not written out the SCET loop integrand, but it follows in a straightforward manner from using the collinear quark and gluon propagators and vertex Feynman rules from Fig. (6). Note that the result for Z_{ξ_n} is the same as the full theory Z_ψ . This occurs because for the wavefunction graph there is no connection

to the ultrasoft modes or the hard production vertex, and by itself a single collinear sector is just a boosted version of full QCD (and Z_ψ is independent of this boost). There are also no subtleties related to zero-bin subtractions for this graph (the subtraction integrands are power suppressed and therefore the subtraction vanishes). There is also a diagram generated by the two-quark two-gluon Feynman rule, but this tadpole type diagram vanishes with our choice of regulators. There is also a tadpole type diagram where two gluons are taken out of the Wilson lines in the vertex, which also vanishes, ie.



$$= 0, \quad = 0. \quad (7.13)$$

The last diagram we must consider is the collinear vertex graph with an attachment from the Wilson line going to the collinear quark propagator,



$$= V_n^1 = -ig^2 C_F \bar{u}_n \Gamma u_v \mu^{2\epsilon} \ell^\epsilon \sum_{\substack{k_\ell \neq 0 \\ k_\ell \neq -p_\ell}} \int \frac{d^d k_r}{(\bar{n} \cdot k_\ell)(k^2)(k+p)^2}$$

$$= -ig^2 C_F \bar{u}_n \Gamma u_v \hat{V}_n^1. \quad (7.14)$$

Here each momentum has been split into label and residual components $k = (k_\ell^\mu, k_r^\mu)$ and $p = (p_\ell^\mu, p_r^\mu)$. There are no +-momenta in the label components, and the only residual component for the external p is its +-momentum. For reasons that will soon become apparent, we have used a short hand notation for the relativistic collinear gluon and quark propagators, which in fact contain a mixture of label and residual momenta,

$$k^2 = k_r^+ k_\ell^- - \vec{k}_\ell^\perp{}^2, \quad (k+p)^2 = (k_r^+ + p_r^+)(k_\ell^- + p_\ell^-) - (\vec{k}_\ell^\perp + \vec{p}_\ell^\perp)^2, \quad (7.15)$$

and are homogeneous in the power counting with $k^2 \sim p^2 \sim \lambda^2$. We have also introduced the notation with a hat, \hat{V}_n^1 , for the collinear loop integrand.

In general in collinear loop integrals there can be a nontrivial interplay between the Wilson coefficients and the large collinear loop integration, because both depend on a momentum that is the same size in the power counting, namely the large minus momenta, $k^- \sim Q$. When matching at one-loop, $\mathcal{O}(\alpha_s)$, in some cases the tree level hard matching coefficient we insert might be independent of the loop momentum k^- . In this case we can insert it back into the calculation only at the end. Even in this case it must be included when considering the renormalization group evolution, because the sharing of large momenta can lead to convolutions in the RG evolution equations. We will meet an example of this type later on when we discuss the running of parton distributions for a collinear proton. For our example of the heavy-to-light current for $b \rightarrow s\gamma$, things are actually simple for a different reason. The SCET operator in Eq. (7.2) contains only a single gauge invariant product of collinear fields, $(\bar{\xi}_n W)$, and the Wilson coefficient only depends on the overall outgoing momentum of this product. Therefore if we include a coefficient into our diagram in Eq. (7.14) it gives only dependence on the total external momentum

$$C[\bar{n} \cdot (p+k) + \bar{n} \cdot (-k)] = C(\bar{n} \cdot p). \quad (7.16)$$

This result remains true for collinear loop diagrams at higher orders, so the coefficient can always be treated as multiplicative for this current, and the coefficient is always evaluated with the total --momentum

of the collinear jet, which in this case is $\bar{n} \cdot p = m_b$. Indeed, even when we have collinear fields for multiple directions, the large momenta are still fixed by the external kinematics *as long as we have only one (gauge invariant product of) collinear fields in each direction*. In this case the Wilson coefficient for the hard dynamics remains multiplicative in momentum space. (And we remark that this is the case that is predominantly studied for amplitudes for LHC processes with an exclusive number of jets. In general the coefficient will still be a matrix in color space once we have enough colored particles to give more than one possibility for making an overall color singlet (4 particles). There is only one possibility for the current example and hence no matrix in color space.) When we have more than one block of gauge invariant collinear fields in the same collinear direction then this will no longer be true, there will be momentum convolutions between the hard coefficient C and the collinear parts of the SCET operator.

To perform the collinear loop integration in Eq. (7.14) we should follow the rules from section 4.5 on combining label and residual momenta. As a first pass we will ignore the 0-bin restrictions $k_\ell \neq 0, -p_\ell$. In this case we can apply the simple rule from Eq. (4.60). Results following this rule in SCET_I are often called the naive collinear integrals. Since only momenta of external collinear particles appear in the loop integrand the multipole expansion is trivial for this integral, and this gives the same result that we would have obtained by ignoring the split into label and residual momenta from the start:

$$\begin{aligned} \hat{V}_n^{1 \text{ naive}} &= \mu^{2\epsilon} \ell^\epsilon \int \frac{\bar{d}^d k (n \cdot \bar{n})(\bar{n} \cdot (p+k))}{(\bar{n} \cdot k) k^2 (k+p)^2} \\ &= \frac{i}{(4\pi)^2} \left[\frac{2}{\epsilon^2} + \frac{2}{\epsilon} + \frac{2}{\epsilon} \ln \left(\frac{\mu^2}{-p^2} \right) + \ln^2 \left(\frac{\mu^2}{-p^2} \right) + 2 \ln \left(\frac{\mu^2}{-p^2} \right) + 4 - \frac{\pi^2}{6} \right]. \end{aligned} \quad (7.17)$$

This result for the loop integral can be obtained either with standard Feynman parameter rules or by contour integration in k^+ or k^- . Feynman parameter tricks and other equations that are useful for doing loop integrals in SCET are summarized in Appendix E.

Having assembled results for all the SCET loop graphs we can now add them up to obtain the bare SCET result

$$\text{Sum SCET} = V_{us}^1 + V_n^1 + \left[\frac{1}{2}(Z_{h_v}^{us} - 1) + \frac{1}{2}(Z_{\xi_n} - 1) \right] V_{\text{scet}}^0, \quad (7.18)$$

and then compare with the full QCD calculation, setting the renormalized coupling $g^2 = 4\pi\alpha_s(\mu)$. For the moment we still will label our SCET result as naive since it ignores the 0-bin restrictions. If we examine the IR divergences encoded in the $\ln(-p^2)$ factors (and the $1/\epsilon_{\text{IR}}$ from the heavy quark wavefunction renormalization) then we find for $\Gamma = P_R i\sigma^{\mu\nu}$ that at leading order $V_{\text{qcd}}^0 = V_{\text{scet}}^0$ and

$$\begin{aligned} (\text{Sum QCD})^{\text{ren}} &= -\frac{\alpha_s C_F}{4\pi} \left[\ln^2 \left(\frac{-p^2}{m_b^2} \right) + \frac{3}{2} \ln \left(\frac{-p^2}{m_b^2} \right) + \frac{1}{\epsilon_{\text{IR}}} + \dots \right] V_{\text{scet}}^0 + \dots, \\ (\text{Sum SCET})^{\text{naive}} &= -\frac{\alpha_s C_F}{4\pi} \left[\ln^2 \left(\frac{-p^2}{m_b^2} \right) + \frac{3}{2} \ln \left(\frac{-p^2}{m_b^2} \right) + \frac{1}{\epsilon_{\text{IR}}} - \frac{1}{\epsilon^2} - \frac{5}{2\epsilon} - \frac{2}{\epsilon} \ln \left(\frac{\mu}{m_b} \right) + \dots \right] V_{\text{scet}}^0. \end{aligned} \quad (7.19)$$

Thus the results match up in the IR (as long as the remaining $1/\epsilon$ terms in the SCET result can be interpreted as UV divergences). To obtain this result for the sum of the SCET diagrams there is an important cancellation between the collinear and ultrasoft diagrams, $\ln(-p^2/\mu^2)/\epsilon - \ln[-p^2/(\mu\bar{n} \cdot p)]/\epsilon = \ln(\bar{n} \cdot p/\mu)/\epsilon = -\ln(\mu/m_b)/\epsilon$. The cancellation of the $\ln(-p^2)$ dependence in this $1/\epsilon$ pole is crucial both to match the IR divergences correctly in QCD, and in order for the remaining $1/\epsilon$ pole to possibly have an ultraviolet interpretation. The remaining dependence on $\bar{n} \cdot p = m_b$ in the $1/\epsilon$ pole is fine because this

is the large momentum that the Wilson coefficient anyway depends on. This same cancellation also has a reflection in the double logarithms where the $\ln(\mu^2)$ dependence cancels out from the $\ln^2(-p^2)$ dependent term. Again this cancellation is important for the matching of IR divergences with the full theory.

The final catch is related to our use of the naive collinear integrand is the interpretation of the $1/\epsilon$ poles from the collinear loop integral. The $1/\epsilon$ divergences from the ultrasoft vertex diagram are clearly determined to be of UV origin (from large euclidean momenta or large light-like momenta). However in the collinear vertex diagram with the naive integral one of the divergences actually comes from $\bar{n} \cdot k \rightarrow 0$, and hence is of IR origin. This IR region is actually already correctly accounted for by the ultrasoft diagram where the heavy quark propagator is time-like, $v \cdot k + i0$, as it should be in the infrared region. In this region the original propagator does not behave like $\bar{n} \cdot k$. The $\bar{n} \cdot k$ term which comes from the collinear Wilson line W is instead the appropriate approximation for large $\bar{n} \cdot k$, rather than small $\bar{n} \cdot k$. Thus the issue with the naive collinear loop integral for the vertex diagram is that it double counts an IR region accounted for by the ultrasoft diagram. This double accounting is removed once we properly consider the 0-bin subtraction contributions. Therefore we apply now the rule with the 0-bin subtractions $k_\ell \neq 0, -p_\ell$ using Eq.(4.64) to obtain

$$\hat{V}_n^1 = \mu^{2\epsilon} \int \bar{d}^d k \left[\frac{(n \cdot \bar{n}) \bar{n} \cdot (p+k)}{(\bar{n} \cdot k) k^2 (k+p)^2} - \frac{(n \cdot \bar{n}) \bar{n} \cdot p}{(\bar{n} \cdot k) k^2 (\bar{n} \cdot p n \cdot k + p^2)} \right] = \hat{V}_n^{1,\text{naive}} - \hat{V}_n^{1,0\text{bin}}. \quad (7.20)$$

It is easy to see where the 0-bin integrand comes from because it can be obtained from the appropriate ultrasoft scaling limit of the naive collinear integrand. For $k_\ell \neq 0$ we have a subtraction for the region $k_\ell \sim \lambda^2$ where we only keep terms up to those scaling as λ^{-8} , which gives precisely the integrand in Eq. (7.20) denoted as $\hat{V}_n^{1,0\text{bin}}$. The terms with $n \cdot k$ and $\bar{n} \cdot k$ in the denominator count as λ^2 , while the term with $k^2 \sim \lambda^4$ to give the eight powers that compensate the $d^d k \sim \lambda^8$ for the subtraction. Note that we have kept the offshellness $0 \neq p^2 \sim \lambda^2$ since it is the same order as the $(\bar{n} \cdot p)(n \cdot k)$ term. The other subtraction is $k_\ell \neq -p_\ell$ so we have the subtraction region $k_\ell + p_\ell \sim \lambda^2$. For this case one of the factors in the denominator is $\bar{n} \cdot k \rightarrow -\bar{n} \cdot p \sim \lambda^0$ (and there is suppression from the numerator as well) so there is no contribution at $\mathcal{O}(\lambda^{-8})$.

Being more careful about the UV ($1/\epsilon$) and IR ($1/\epsilon_{\text{IR}}$) divergences we find

$$\begin{aligned} \hat{V}_n^{1,\text{naive}} &= \frac{i}{(4\pi)^2} \left[\frac{2}{\epsilon_{\text{IR}} \epsilon} + \frac{2}{\epsilon} + \frac{2}{\epsilon_{\text{IR}}} \ln \frac{\mu^2}{-p^2} + \left(\frac{2}{\epsilon} - \frac{2}{\epsilon_{\text{IR}}} \right) \ln \frac{\mu}{\bar{n} \cdot p} + \ln^2 \frac{\mu^2}{-p^2} + 2 \ln \frac{\mu^2}{-p^2} + 4 - \frac{\pi^2}{6} \right], \\ \hat{V}_n^{1,0\text{bin}} &= \frac{i}{(4\pi)^2} \left[\frac{2}{\epsilon} - \frac{2}{\epsilon_{\text{IR}}} \right] \left[\frac{1}{\epsilon} + \ln \frac{\mu^2}{-p^2} - \ln \frac{\mu}{\bar{n} \cdot p} \right], \\ V_n^1 &= \frac{\alpha_s C_F}{4\pi} \left[\frac{2}{\epsilon^2} + \frac{2}{\epsilon} + \frac{2}{\epsilon} \ln \left(\frac{\mu^2}{-p^2} \right) + \ln^2 \left(\frac{\mu^2}{-p^2} \right) + 2 \ln \left(\frac{\mu^2}{-p^2} \right) + 4 - \frac{\pi^2}{6} \right]. \end{aligned} \quad (7.21)$$

So we see that the subtraction cancels the $\bar{n} \cdot q \rightarrow 0$ IR singularities $1/\epsilon_{\text{IR}}$ in the first line. The UV divergences arising from $\bar{n} \cdot q \rightarrow \infty$ are independent of the IR regulator and just depend on the UV regulator ϵ . Since the 0-bin contribution is scaleless with our choice of regulators, taking $\epsilon_{\text{IR}} = \epsilon$ and ignoring this subtraction would give us the correct answer. Nevertheless, even with this regulator the 0-bin contribution is still important to obtain the correct physical interpretation for the divergences.⁶

Since the final result after subtracting the 0-bin contribution is the same as in Eq. (7.17) with the $1/\epsilon$ poles all now known to be UV, we can determine the appropriate UV counterterm to renormalize the SCET current. Defining

$$C^{\text{bare}}(\omega, \epsilon) = Z_C(\mu, \omega, \epsilon) C(\mu, \omega) = C + (Z_C - 1)C, \quad (7.22)$$

⁶For other less inclusive calculations or for other choices of regulators (such as $\Omega_\perp^2 \leq \vec{k}_\perp^2 \leq \Lambda_\perp^2$, $\Omega_\perp^2 \leq (k^-)^2 \leq \Lambda_\perp^2$) the subtractions are even more crucial to obtain the correct result and have the UV divergences independent of the IR regulator.

and adding the counterterm graph with $(Z_C - 1)C$ to cancel the $1/\epsilon$ poles in $\overline{\text{MS}}$ gives

$$Z_C(\mu, \omega, \epsilon) = 1 - \frac{C_F \alpha_s(\mu)}{4\pi} \left(\frac{1}{\epsilon^2} + \frac{1}{\epsilon} \ln \frac{\mu^2}{\omega^2} + \frac{5}{2\epsilon} \right) + \mathcal{O}(\alpha_s^2). \quad (7.23)$$

(Where by momentum conservation $\omega = m_b$.) We can now add up the collinear and ultrasoft loop graphs to obtain the final renormalized SCET result, and compare with the renormalized QCD result

$$\begin{aligned} (\text{Sum QCD})^{\text{ren}} &= -\frac{\alpha_s C_F}{4\pi} \left[\frac{1}{\epsilon_{\text{IR}}} + \ln^2 \left(\frac{-p^2}{\omega^2} \right) + \frac{3}{2} \ln \left(\frac{-p^2}{\omega^2} \right) + 2 \ln \left(\frac{\mu}{\omega} \right) + f_1 \left(\frac{\omega}{m_b} \right) + \frac{5}{2} \right] V_{\text{scet}}^0 \\ &\quad + \frac{\alpha_s C_F}{4\pi} f_2 \left(\frac{\omega}{m_b} \right) \bar{u}_s P_R \left(\frac{p^\mu \gamma^\nu - p^\nu \gamma^\mu}{m_b} \right) u_b, \\ (\text{Sum SCET})^{\text{ren}} &= V_{us}^1 + V_n^1 + \left[\frac{1}{2} (Z_{h_v}^{us} - 1) + \frac{1}{2} (Z_{\xi_n} - 1) + (Z_C - 1) \right] V_{\text{scet}}^0 \\ &= -\frac{\alpha_s C_F}{4\pi} \left[\frac{1}{\epsilon_{\text{IR}}} + \ln^2 \left(\frac{-p^2}{\omega^2} \right) + \frac{3}{2} \ln \left(\frac{-p^2}{\mu^2} \right) - 2 \ln^2 \left(\frac{\mu}{\omega} \right) + \frac{11\pi^2}{12} - \frac{7}{2} \right] V_{\text{scet}}^0. \end{aligned} \quad (7.24)$$

From these two results we see that the renormalized QCD and SCET have the same infrared divergences. The difference of these results is determined by ultraviolet physics and determines the one-loop matching result for the $\overline{\text{MS}}$ Wilson coefficients $C_1(\mu, \omega, m_b)$ and $C_2(\mu, \omega, m_b)$ that multiply the SCET operator in Eq. (7.2) for the Dirac structures $\Gamma = \Gamma_1 = P_R i \sigma^{\mu\nu}$ and $\Gamma = \Gamma_2 = P_R (n^\mu \gamma_\perp^\nu - n^\nu \gamma_\perp^\mu)$ respectively. Only the Dirac structure Γ_1 was present at tree-level, while Γ_2 is generated at one-loop. Taking the difference of the above two results and simplifying we find

$$\begin{aligned} C_1(\mu, \omega, m_b) &= 1 - \frac{C_F \alpha_s(\mu)}{4\pi} \left[2 \ln^2 \left(\frac{\mu}{\omega} \right) + 5 \ln \left(\frac{\mu}{\omega} \right) + f_1 \left(\frac{\omega}{m_b} \right) - \frac{11\pi^2}{12} + 6 \right], \\ C_2(\mu, \omega, m_b) &= \frac{C_F \alpha_s(\mu)}{4\pi} \frac{\omega}{2m_b} f_2 \left(\frac{\omega}{m_b} \right). \end{aligned} \quad (7.25)$$

7.2 $e^+e^- \rightarrow 2\text{-jets}$, SCET Loops

In this section we perform the matching from QCD onto SCET for the process $e^+e^- \rightarrow 2\text{-jets}$. This matching will be independent of the details of the kinematical constraints that are used to enforce that we really are restricting ourselves to have only 2 jets in the final state, which will all be contained in the long distance dynamics of the effective theory. Indeed, the fact that we can successfully carry out this matching at the amplitude level makes it clear that it does not depend on which constraints we put on the phase space of the 2-jet final state. Once again, it will also be independent of the choice of IR regulator as long as the same regulator is used in both the QCD and SCET calculations. We will use Feynman gauge in both QCD and SCET, and take $d = 4 - 2\epsilon$ to regulate UV divergences and offshellness for the quark and antiquark, $p_q^2 = p_{\bar{q}}^2 = p^2 \neq 0$, to regulate all IR divergences.

In full QCD, the production of hadrons in e^+e^- collisions occurs via an s-channel exchange of a virtual photon or a Z boson. The coupling is either via a vector or an axial vector current and is therefore given by

$$J^{\text{QCD}} = \bar{q} \Gamma_i q, \quad \Gamma_V = g_V \gamma^\mu, \quad \Gamma_A = g_A \gamma^\mu \gamma^5, \quad (7.26)$$

where $g_{V,A}$ contain the electroweak couplings for the photon or Z -boson (for a virtual photon $g_V = e_q$ the electromagnetic charge of the quark q , and $g_A = 0$). In SCET the current involves collinear quarks in the

back-to-back n and \bar{n} directions

$$J^{\text{SCET}} = (\bar{\xi}_{\bar{n}} W_{\bar{n}}) \Gamma_i C(\mathcal{P}_{\bar{n}}^\dagger, \mathcal{P}_n, \mu) (W_n^\dagger \xi_n) = \int d\omega d\omega' C(\omega, \omega') \bar{\chi}_{\bar{n}, \omega'} \Gamma_i \chi_{n, \omega}. \quad (7.27)$$

By reparametrization invariance of type-III the dependence on the label operators can only be in the combination $\omega\omega'$ inside C , so

$$C(\omega, \omega') = C(\omega\omega'). \quad (7.28)$$

Finally in the CM frame momentum conservation fixes $\omega = \omega' = Q$, the CM energy of the e^+e^- pair, so we can write

$$J^{\text{SCET}} = C(Q^2) (\bar{\xi}_{\bar{n}} W_{\bar{n}}) \Gamma_i (W_n^\dagger \xi_n), \quad (7.29)$$

and the matching calculation in this section will determine the renormalized $\overline{\text{MS}}$ Wilson coefficient $C(Q^2, \mu^2)$. In this case there is only one relevant Dirac structure Γ_i in SCET for each of the vector and axial-vector currents.

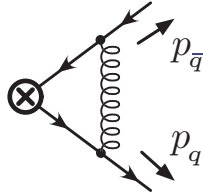
We again begin by calculating the full theory diagrams. As in the case of $B \rightarrow X_s \gamma$ we need the wave function contributions for the light quarks, in this case one for the quark and one for the anti-quark. Both wave function contributions are the same as the results obtained before

$$Z_\psi = 1 - \frac{\alpha_s C_F}{4\pi} \left[\frac{1}{\epsilon} - \ln \frac{-p^2}{\mu^2} + 1 \right]. \quad (7.30)$$

The remaining vertex graph can again be calculated in a straightforward manner. At tree level we find

$$V_{\text{qcd}}^0 = \bar{u}(p_n) \Gamma_i v_{\bar{n}}(p_{\bar{n}}) \quad (7.31)$$

while the one loop vertex diagram



gives

$$\begin{aligned} V_{\text{qcd}}^1 &= \mu^{2\epsilon} \iota^\epsilon \int \frac{d^d k}{(2\pi)^d} ig \bar{u}(p_q) \gamma^\alpha T^A \frac{i(\not{p}_q + \not{k})}{(p_q + k)^2} \Gamma_i \frac{-i(\not{p}_{\bar{q}} + \not{k})}{(p_{\bar{q}} + k)^2} ig \gamma_\alpha T^A v(p_{\bar{q}}) \frac{-i}{k^2} \\ &= ig^2 C_F \mu^{2\epsilon} \int \frac{d^d k}{(2\pi)^d} \bar{u}(p_q) \frac{\gamma^\alpha (\not{p}_q + \not{k}) \Gamma_i (\not{p}_{\bar{q}} + \not{k}) \gamma_\alpha}{(p_q + k)^2 (p_{\bar{q}} + k)^2 k^2} v(p_{\bar{q}}) \\ &= \frac{\alpha_s C_F}{4\pi} \left[\frac{1}{\epsilon} - 2 \ln^2 \frac{p^2}{Q^2} - 5 \ln \frac{p^2}{Q^2} - 2 \ln \frac{(-Q^2 - i0)}{\mu^2} - \frac{2\pi^2}{3} + 1 \right] \bar{u}(p_q) \Gamma_i v(p_{\bar{q}}). \quad (7.32) \end{aligned}$$

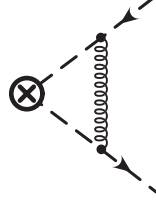
Here $\iota^\epsilon = (4\pi)^{-\epsilon} e^{\epsilon\gamma_E}$ ensures that the scale μ has the appropriate normalization for the $\overline{\text{MS}}$ scheme. Adding the QCD diagrams we find

$$\begin{aligned} \text{QCD Sum} &= V_{\text{qcd}}^1 + 2 \left[\frac{1}{2} (Z_\psi - 1) \right] V_{\text{qcd}}^0 \\ &= \frac{\alpha_s C_F}{4\pi} \left[-2 \ln^2 \frac{p^2}{Q^2} - 4 \ln \frac{p^2}{Q^2} - \ln \frac{-Q^2}{\mu^2} - \frac{2\pi^2}{3} \right] \bar{u}(p_q) \Gamma_i v(p_{\bar{q}}). \quad (7.33) \end{aligned}$$

As before, we next consider the loops in SCET. The wave function renormalization for the collinear quark is the same as in the previous section, and we find

$$Z_\xi^{us} = 0, \quad Z_\xi = 1 - \frac{C_F \alpha_s}{4\pi} \left(\frac{1}{\epsilon} - \ln \frac{-p^2}{\mu^2} + 1 \right). \quad (7.34)$$

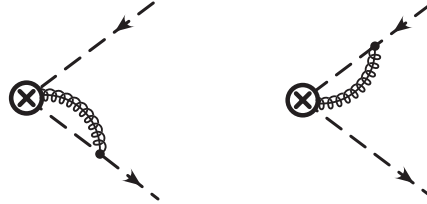
The tree level amplitude in SCET is $V_{\text{scet}}^0 = \bar{u}_n(p_q) \Gamma_i v_{\bar{n}}(p_{\bar{q}})$, and to leading order $V_{\text{qcd}}^0 = V_{\text{scet}}^0$. The ultrasoft vertex graph in SCET involves an exchange between the n -collinear and \bar{n} -collinear quarks,



and is given by

$$\begin{aligned} V_{\text{usoft}}^1 &= \mu^{2\epsilon} \ell^\epsilon \int \frac{d^d k}{(2\pi)^d} \bar{u}_n \left(ig \frac{\not{n}}{2} n^\alpha T^A \right) \frac{i \not{n}}{2} \frac{\bar{n} \cdot p_q}{\bar{n} \cdot p_q} \frac{1}{n \cdot k + p_q^2} \Gamma_i \frac{i \not{n}}{2} \frac{-n \cdot p_{\bar{q}}}{n \cdot p_{\bar{q}}} \frac{1}{\bar{n} \cdot k + p_{\bar{q}}^2} \left(ig \frac{\not{n}}{2} \bar{n}_\alpha T^A \right) v_{\bar{n}} \frac{-i}{k^2} \\ &= ig^2 C_F \mu^{2\epsilon} \ell^\epsilon \left(\bar{u}_n \frac{\not{n} \not{\bar{n}}}{4} \Gamma_i \frac{\not{\bar{n}} \not{n}}{4} v_{\bar{n}} \right) \int \frac{d^d k}{(2\pi)^d} \frac{n \cdot \bar{n}}{\left(n \cdot k + \frac{p_q^2}{\bar{n} \cdot p_q} \right) \left(\bar{n} \cdot k + \frac{p_{\bar{q}}^2}{n \cdot p_{\bar{q}}} \right) k^2} \\ &= \frac{\alpha_s C_F}{4\pi} \left[-\frac{2}{\epsilon^2} + \frac{2}{\epsilon} \ln \frac{-p^4}{\mu^2 Q^2} - \ln^2 \frac{-p^4}{\mu^2 Q^2} - \frac{\pi^2}{2} \right] \bar{u}_n(p_q) \Gamma_i v_{\bar{n}}(p_{\bar{q}}). \end{aligned} \quad (7.35)$$

There are two possible collinear vertex graphs which involve a contraction between the $W_n[\bar{n} \cdot A_n]$ Wilson line and a n -collinear quark, and another between the $W_{\bar{n}}[n \cdot A_{\bar{n}}]$ Wilson line and the \bar{n} -collinear quark



For the first diagram, we find

$$\begin{aligned} V_{\text{coll}}^1 &= \mu^{2\epsilon} \ell^\epsilon \int \frac{d^d k}{(2\pi)^d} ig \bar{u}_n \left[n^\alpha + \frac{\gamma^\perp \not{p}_\perp}{\bar{n} \cdot p} + \frac{(\not{p}_\perp + \not{k}_\perp) \gamma_\perp^\alpha}{\bar{n} \cdot (p+k)} - \frac{\not{p}_\perp (\not{p}_\perp + \not{k}_\perp)}{\bar{n} \cdot p \bar{n} \cdot (p+k)} \right] \frac{\not{n}}{2} T^A \\ &\quad \times i \frac{\not{n}}{2} \frac{\bar{n} \cdot (p+k)}{(p+k)^2} \left(-g \frac{\bar{n}_\alpha}{\bar{n} \cdot k} T^A \right) \frac{-i}{k^2} \Gamma_i v_{\bar{n}} \\ &= -ig^2 C_F \mu^{2\epsilon} \ell^\epsilon \int \frac{d^d k}{(2\pi)^d} \frac{(n \cdot \bar{n}) \bar{n} \cdot (p+k)}{\bar{n} \cdot k (p+k)^2 k^2} \bar{u}_n \Gamma_i v_{\bar{n}} \\ &= \frac{\alpha_s C_F}{4\pi} \left[\frac{2}{\epsilon^2} + \frac{2}{\epsilon} - \frac{2}{\epsilon} \ln \frac{-p^2}{\mu^2} + \ln^2 \frac{-p^2}{\mu^2} - 2 \ln \frac{-p^2}{\mu^2} + 4 - \frac{\pi^2}{6} \right] \bar{u}_n(p_q) \Gamma_i v_{\bar{n}}(p_{\bar{q}}). \end{aligned} \quad (7.36)$$

One can easily show that the second collinear vertex diagram gives the same result as the first diagram. Furthermore the collinear integral here is identical to the one for $b \rightarrow s\gamma$ in Eq. (7.14). The result in Eq. (7.36) is for the naive integrand, since it does not include the 0-bin subtraction contribution. But the

0-bin subtraction terms here are scaleless as in Eq. (7.21), and hence the final result in Eq. (7.36) is correct with the interpretation of the $1/\epsilon$ divergences as UV.

Adding the SCET diagrams we find after some straightforward manipulations

$$\begin{aligned} \text{SCET Sum} &= V_{\text{usoft}}^1 + 2V_{\text{coll}}^1 + 2\left[\frac{1}{2}(Z_\xi - 1)\right]V_{\text{scet}}^0 \\ &= \frac{\alpha_s C_F}{4\pi} \left[\frac{2}{\epsilon^2} + \frac{3}{\epsilon} - \frac{2}{\epsilon} \ln \frac{-Q^2}{\mu^2} + 2 \ln^2 \frac{\mu^2}{-p^2} - \ln^2 \frac{\mu^2 Q^2}{-p^4} + 4 \ln \frac{\mu^2}{-p^2} + 8 - \frac{5\pi^2}{6} \right] \bar{u}_n \Gamma_i v_{\bar{n}} \\ &= \frac{\alpha_s C_F}{4\pi} \left[\frac{2}{\epsilon^2} + \frac{3}{\epsilon} - \frac{2}{\epsilon} \ln \frac{-Q^2}{\mu^2} - 2 \ln^2 \frac{p^2}{Q^2} + \ln^2 \frac{-Q^2}{\mu^2} - 4 \ln \frac{p^2}{Q^2} - 4 \ln \frac{-Q^2}{\mu^2} + 8 - \frac{5\pi^2}{6} \right] \bar{u}_n \Gamma_i v_{\bar{n}}. \end{aligned} \quad (7.37)$$

Comparing the $\ln(p^2)$ dependence in the final line to the QCD amplitude in Eq. (7.33) We can see that SCET reproduces all IR divergences of the form $\ln p^2/Q^2$, and that the matching coefficient is therefore independent of IR divergences as it should. However, while the matrix element of the full QCD current is UV finite (since it is a conserved current), the matrix element in the effective theory is UV divergent and therefore needs to be renormalized. Defining a renormalized coupling by

$$C(Q, \epsilon) = Z_C(\mu, Q, \epsilon)C(\mu, Q) = C + (Z_C - 1)C \quad (7.38)$$

the renormalization constant that cancels the divergences in Eq. (7.37) is

$$Z_C = 1 + \frac{C_F \alpha_s(\mu)}{4\pi} \left[-\frac{2}{\epsilon^2} - \frac{3}{\epsilon} + \frac{2}{\epsilon} \ln \left(\frac{-Q^2 - i0}{\mu^2} \right) \right]. \quad (7.39)$$

Taking the difference between the renormalized matrix elements in full QCD and SCET,

$$\begin{aligned} (\text{QCD sum})^{\text{ren}} &= \frac{\alpha_s C_F}{4\pi} \left[-2 \ln^2 \frac{p^2}{Q^2} - 4 \ln \frac{p^2}{Q^2} - \ln \frac{-Q^2}{\mu^2} - \frac{2\pi^2}{3} \right] \bar{u}(p_n) \Gamma_i v(p_{\bar{n}}), \\ (\text{SCET sum})^{\text{ren}} &= \frac{\alpha_s C_F}{4\pi} \left[-2 \ln^2 \frac{p^2}{Q^2} + \ln^2 \frac{-Q^2}{\mu^2} - 4 \ln \frac{p^2}{Q^2} - 4 \ln \frac{-Q^2}{\mu^2} + 8 - \frac{5\pi^2}{6} \right] \bar{u}_n \Gamma_i v_{\bar{n}}, \end{aligned} \quad (7.40)$$

we obtain the matching result for Wilson coefficient of the operator in Eq. (7.29) at one-loop order

$$C(\mu, Q) = 1 + \frac{C_F \alpha_s(\mu)}{4\pi} \left[-\ln^2 \left(\frac{-Q^2 - i0}{\mu^2} \right) + 3 \ln \left(\frac{-Q^2 - i0}{\mu^2} \right) - 8 + \frac{\pi^2}{6} \right]. \quad (7.41)$$

Note that the only momentum dependence in the Wilson coefficient is in logarithms of the ratio of the renormalization scale to the hard scale Q . This dependence signals that it captures offshell physics from the hard scale Q that we are integrating out. If we choose the renormalization scale to be equal to Q , we find that all logarithms vanish

$$C(Q, Q) = 1 + \frac{C_F \alpha_s(Q)}{4\pi} \left[-8 + \frac{7\pi^2}{6} - 3i\pi \right]. \quad (7.42)$$

Sometimes it is useful to avoid inducing large factors of π in the non-logarithmic terms, which can be accomplished by using a complex scale, $\mu = -iQ$. Here this gives

$$C(-iQ, Q) = 1 + \frac{C_F \alpha_s(-iQ)}{4\pi} \left[-8 + \frac{\pi^2}{6} \right]. \quad (7.43)$$

For dijet observables described by the current in Eq. (7.29) the cross section is obtained by squaring the amplitude, and will depend on a hard function defined by

$$H(\mu, Q) = |C(\mu, Q)|^2. \quad (7.44)$$

Thus the imaginary contributions in $C(\mu, Q)$ cancel out for these observables.

7.3 Summing Sudakov Logarithms

With the information from either of the last two sections, we can calculate the anomalous dimensions of the operators or Wilson coefficients. Taking

$$0 = \mu \frac{d}{d\mu} C^{\text{bare}}(\epsilon) = \mu \frac{d}{d\mu} [Z_C(\mu, \epsilon) C(\mu)] = \left[\mu \frac{d}{d\mu} Z_C(\mu, \epsilon) \right] C(\mu) + Z_C(\mu, \epsilon) \left[\mu \frac{d}{d\mu} C(\mu) \right], \quad (7.45)$$

we see that the anomalous dimension is defined by a derivative of the counterterm

$$\mu \frac{d}{d\mu} C(\mu) = \left[-Z_C^{-1}(\mu, \epsilon) \mu \frac{d}{d\mu} Z_C(\mu, \epsilon) \right] C(\mu) \equiv \gamma_C(\mu) C(\mu). \quad (7.46)$$

To calculate the μ derivative we should recall the result for the derivative of the strong coupling in d dimensions

$$\mu \frac{d}{d\mu} \alpha_s(\mu, \epsilon) = -2\epsilon \alpha_s(\mu, \epsilon) + \beta[\alpha_s], \quad (7.47)$$

where $\beta[\alpha_s]$ is the standard $d = 4$ QCD beta function written in terms of $\alpha_s(\mu, \epsilon)$.

Lets apply this to our two examples in turn. The counterterm for the $b \rightarrow s\gamma$ current is

$$Z_C^\gamma = 1 - \frac{\alpha_s(\mu) C_F}{4\pi} \left(\frac{1}{\epsilon^2} + \frac{2}{\epsilon} \ln \frac{\mu}{\omega} + \frac{5}{2\epsilon} \right). \quad (7.48)$$

Using the definition of γ_C in Eq. (7.46) we find

$$\begin{aligned} \gamma_C^\gamma(\mu, \omega, \epsilon) &= -\frac{1}{Z_C^\gamma} \mu \frac{d}{d\mu} Z_C^\gamma = \mu \frac{d}{d\mu} \frac{C_F \alpha_s(\mu, \epsilon)}{4\pi} \left(\frac{1}{\epsilon^2} + \frac{2}{\epsilon} \ln \frac{\mu}{\omega} + \frac{5}{2\epsilon} \right) \\ &= \frac{C_F \alpha_s(\mu, \epsilon)}{4\pi} \left(-\frac{2}{\epsilon} - 4 \ln \frac{\mu}{\omega} - 5 + \frac{2}{\epsilon} \right) + \mathcal{O}(\alpha_s^2), \\ \gamma_C^\gamma(\mu, \omega) &= -\frac{\alpha_s(\mu)}{4\pi} \left(4C_F \ln \frac{\mu}{\omega} + 5C_F \right), \end{aligned} \quad (7.49)$$

where we differentiated both $\alpha_s(\mu)$ and the explicit $\ln(\mu)$, noting that the $1/\epsilon$ terms cancel to yield a well defined anomalous dimension in the $\epsilon \rightarrow 0$ limit which is given on the last line.

Similarly, the counterterm for the $e^+e^- \rightarrow \text{dijets}$ current is

$$Z_C^{2\text{jet}} = 1 + \frac{C_F \alpha_s(\mu)}{4\pi} \left[-\frac{2}{\epsilon^2} - \frac{3}{\epsilon} + \frac{2}{\epsilon} \ln \left(\frac{-Q^2 - i0}{\mu^2} \right) \right], \quad (7.50)$$

so the anomalous dimension is obtained by

$$\begin{aligned} \gamma_C^{2\text{jet}}(\mu, Q, \epsilon) &= -\frac{1}{Z_C^{2\text{jet}}} \mu \frac{d}{d\mu} Z_C^{2\text{jet}} = \mu \frac{d}{d\mu} \frac{C_F \alpha_s(\mu, \epsilon)}{4\pi} \left[\frac{2}{\epsilon^2} + \frac{3}{\epsilon} + \frac{2}{\epsilon} \ln \left(\frac{\mu^2}{-Q^2 - i0} \right) \right] \\ &= \frac{C_F \alpha_s(\mu, \epsilon)}{4\pi} \left[\frac{-4}{\epsilon} - 6 - 4 \ln \left(\frac{\mu^2}{-Q^2 - i0} \right) + \frac{4}{\epsilon} \right] + \mathcal{O}(\alpha_s^2), \\ \gamma_C^{2\text{jet}}(\mu, Q) &= -\frac{\alpha_s(\mu)}{4\pi} \left[4C_F \ln \left(\frac{\mu^2}{-Q^2 - i0} \right) + 6C_F \right]. \end{aligned} \quad (7.51)$$

Again in the last line we have taken the $\epsilon \rightarrow 0$ limit. Note the similarity in the form of the anomalous dimensions for our two examples of Wilson coefficients. Both anomalous dimension equations for $C(\mu)$ are homogeneous linear differential equations because in both cases the operator mixes back into itself.

An interesting feature of anomalous dimensions in SCET is the presence of a single logarithm, $\ln(\mu)$. It can be shown by the consistency of SCET, or by consistency of top-down versus bottom-up evolution using a factorization theorem for a process with Sudakov logarithms, that no terms with more than a single logarithm can appear in anomalous dimensions. The coefficient of this single logarithm is related to the cusp anomalous dimension that governs the renormalization of Wilson lines that meet at a cusp angle β_{ij} between lines along the four vectors n_i and n_j , where $\cosh \beta_{ij} = n_i \cdot n_j / [|n_i| |n_j|]$. In the light-like limit $n_i^2, n_j^2 \rightarrow 0$ we have $\beta_{ij} \rightarrow \infty$. The cusp anomalous dimension is linear in β_{ij} in this limit, which yields a logarithmic dependence on $2n_i \cdot n_j / [|n_i| |n_j|]$ since $\cosh \beta_{ij} \simeq e^{\beta_{ij}}/2$. This single logarithm is the same one encountered in Eqs. (7.49) and (7.50), where the divergence has been handled by the renormalization procedure, and hence has become a $\ln(\mu)$. Indeed, if we consider making the BPS field redefinition for the dijet current we get $Y_n^\dagger Y_{\bar{n}}$, so it is clear that our ultrasoft diagrams involve two light-like Wilson lines meeting at a cusp. In the case of the collinear diagrams we have a Wilson line W_n that meets up with a collinear quark ξ_n , and in doing so also effectively forms a cusp.

The all orders form for the anomalous dimension of our two example currents is

$$\begin{aligned} \gamma_C(\mu, \omega) &= -a_C \Gamma_{\text{cusp}}[\alpha_s(\mu)] \ln\left(\frac{\mu}{\omega_C}\right) - \gamma_C[\alpha_s(\mu)], \\ \Gamma_{\text{cusp}}[\alpha_s] &= \sum_{k=1}^{\infty} \left(\frac{\alpha_s}{4\pi}\right)^k \Gamma_k^{\text{cusp}}, \quad \gamma_C[\alpha_s] = \sum_{k=1}^{\infty} \left(\frac{\alpha_s}{4\pi}\right)^k \gamma_k^C, \end{aligned} \quad (7.52)$$

where $\Gamma_{\text{cusp}}[\alpha_s]$ is called the cusp-anomalous dimension, and the one-loop result has $\Gamma_1^{\text{cusp}} = 4$. The constant prefactor a_C , the dimensionful variable ω_C , and the non-cusp anomalous dimension $\gamma_C[\alpha_s]$ all depend on the particular current under consideration. In order to solve the anomalous dimension equation we should decide what terms must be kept at each order in perturbation theory that we would like to consider. Counting $\alpha_s \ln(\mu) \sim 1$, the correct grouping for obtaining the leading-log (LL), next-to-leading log (NLL), etc., results is

$$\gamma_C(\mu, \omega) \sim [\alpha_s \ln(\mu)]_{\text{LL}} + [\alpha_s + \alpha_s^2 \ln(\mu)]_{\text{NLL}} + [\alpha_s^2 + \alpha_s^3 \ln(\mu)]_{\text{NNLL}} + \dots \quad (7.53)$$

Thus we see that the cusp-anomalous dimension with the $\ln(\mu)$ is required at one-higher order than the non-cusp anomalous dimension. (Typically this is not a problem due to the universal form of the cusp contribution, and the fact that its coefficients are known to 3-loop order for QCD, that is up to Γ_3^{cusp} .) To solve the first order differential equation involving γ_C we also must specify a boundary condition for $C(\mu, \omega)$. At both LL and NLL order the tree-level boundary condition suffices, while at NNLL we need the one-loop boundary condition, etc.

Lets solve the generic anomalous dimension at LL order where

$$\mu \frac{d}{d\mu} \ln C(\mu, \omega) = -4a_C \frac{\alpha_s(\mu)}{4\pi} \ln\left(\frac{\mu}{\omega}\right) = -\frac{a_C \alpha_s(\mu)}{\pi} \ln\left(\frac{\mu}{\omega}\right). \quad (7.54)$$

This equation may be solved for specific quantum field theories. For QED without massless fermions the coupling does not run, and with the tree-level boundary condition $C(\mu = \omega, \omega) = 1 + \mathcal{O}(\alpha_s)$ we have

$$C(\mu, \omega) = \exp\left[-a_C \frac{\alpha}{2\pi} \ln^2\left(\frac{\mu}{\omega}\right)\right]. \quad (7.55)$$

This result involves an exponential of a double logarithm, and is often referred to as the Sudakov form factor. The suppression encoded in this result is related to the restrictions in phase space that are intrinsic for the allowed types of radiation that our operators can emit. The Sudakov form factor also gives the

probability of evolving without branching in a parton shower. For QCD we must also account for the running of the coupling, and at LL order we can use the LL β -function,

$$\mu \frac{d}{d\mu} \alpha_s(\mu) = -\frac{\beta_0}{2\pi} \alpha_s^2(\mu), \quad \beta_0 = \frac{11}{3} C_A - \frac{4}{3} T_F n_f. \quad (7.56)$$

Together Eqs. (7.54) and (7.56) are a coupled set of differential equations. The easiest way to solve these two equations is to use the second one to implement a change of variable for the first by noting that

$$d \ln \mu = \frac{d\alpha_s}{\beta[\alpha_s]} = -\frac{2\pi}{\beta_0} \frac{d\alpha_s}{\alpha_s^2}, \quad \ln\left(\frac{\mu}{\omega}\right) = -\frac{2\pi}{\beta_0} \int_{\alpha_s(\omega)}^{\alpha_s(\mu)} \frac{d\alpha}{\alpha^2}. \quad (7.57)$$

Using the more generic boundary condition which fixes the coefficient at the scale μ_0 , $C(\mu_0, \omega) = 1 + \mathcal{O}(\alpha_s)$ we then have

$$\begin{aligned} \ln C(\mu, \omega) &= -\left(\frac{2\pi}{\beta_0}\right)^2 \int_{\alpha_s(\mu_0)}^{\alpha_s(\mu)} \frac{d\alpha_s}{\alpha_s^2} \frac{a_C \alpha_s}{\pi} \int_{\alpha_s(\omega)}^{\alpha_s} \frac{d\alpha}{\alpha^2} \\ &= -\frac{4\pi a_C}{\beta_0^2} \int_{\alpha_s(\mu_0)}^{\alpha_s(\mu)} \frac{d\alpha_s}{\alpha_s} \left[-\frac{1}{\alpha_s} + \frac{1}{\alpha_s(\omega)} \right] \\ &= -\frac{4\pi a_C}{\beta_0^2} \left[\frac{1}{\alpha_s(\mu)} - \frac{1}{\alpha_s(\mu_0)} + \frac{1}{\alpha_s(\omega)} \ln\left(\frac{\alpha_s(\mu)}{\alpha_s(\mu_0)}\right) \right] \\ &= -\frac{4\pi a_C}{\beta_0^2 \alpha_s(\mu_0)} \left(\frac{1}{z} - 1 + \ln z \right) - \frac{2a_C}{\beta_0} \ln\left(\frac{\omega}{\mu_0}\right) \ln z, \end{aligned} \quad (7.58)$$

where in the last line we used $1/\alpha_s(\omega) = 1/\alpha_s(\mu_0) + \frac{\beta_0}{2\pi} \ln(\omega/\mu_0)$, and defined

$$z \equiv \frac{\alpha_s(\mu)}{\alpha_s(\mu_0)}. \quad (7.59)$$

The solution is therefore

$$C(\mu, \omega) = \exp \left[-\frac{4\pi a_C}{\beta_0^2 \alpha_s(\mu_0)} \left(\frac{1}{z} - 1 + \ln z \right) \right] \left(\frac{\omega}{\mu_0} \right)^{-2a_C \ln z / \beta_0}. \quad (7.60)$$

This result sums the infinite tower of leading-logarithms in the exponent which are of the form, $C \sim \exp(-\alpha_s L^2 - \alpha_s^2 L^3 - \alpha_s^3 L^4 - \dots)$, where the coefficients here are schematic and $L = \ln(\mu/\mu_0)$ is a potentially large logarithm. Again this result is called the Sudakov form factor with a running coupling. Note that the form of the series obtained by expanding in the argument of the exponent is much simpler than what we would obtain by expanding the exponent itself. At each order in resummed perturbation theory the terms that are determined by solving the anomalous dimension equation can be classified by the simpler series that appears in the exponential as follows

$$\ln C \sim \left[-L \sum_k (\alpha_s L)^k \right]_{\text{LL}} + \left[\sum_k (\alpha_s L)^k \right]_{\text{NLL}} + \left[\sum_k \alpha_s (\alpha_s L)^k \right]_{\text{NNLL}} + \dots \quad (7.61)$$

A natural question to ask is how generic are the two examples treated so far in this section? It turns out that much of the structure here is quite generic for cases like our examples, where the ω variables are fixed by external kinematics. This will occur for any operator that involves only one building block, χ_n or $\mathcal{B}_{n\perp}^\mu$, for each collinear direction n . For example, with four collinear directions we have the operator

$$\int d\omega_1 d\omega_2 d\omega_3 d\omega_4 C(\omega_1, \omega_2, \omega_3, \omega_4) \left[\bar{\chi}_{n_1, \omega_1} \Gamma_{\mu\nu} \mathcal{B}_{n_2\perp, \omega_2}^\mu \mathcal{B}_{n_3\perp, \omega_3}^\nu \chi_{n_4, \omega_4} \right] \quad (7.62)$$

MIT OpenCourseWare
<http://ocw.mit.edu>

8.851 Effective Field Theory
Spring 2013

For information about citing these materials or our Terms of Use, visit: <http://ocw.mit.edu/terms>.